Syntheses, Crystal Structures, and Properties of New Layered Molybdenum(VI) Selenites: $(NH_4)_2(MoO_3)_3SeO_3$ and $Cs_2(MoO_3)_3SeO_3$

William T. A. Harrison, Laurie L. Dussack, and Allan J. Jacobson*

Department of Chemistry, University of Houston, Houston, Texas 77204-5641

Received May 20, 1994[⊗]

The hydrothermal syntheses, single-crystal structures, and some properties of two new layered molybdenum selenites, $(NH_4)_2(MoO_3)_3SeO_3$ and $Cs_2(MoO_3)_3SeO_3$, are described. These phases are built up from infinite, hexagonal tungsten bronze-like, anionic layers of MoO_6 octahedra, capped on one side by pyramidally-coordinated Se atoms. The molybdenum-oxygen octahedra show an unusual distortion of the Mo atom towards an octahedral face, resulting in a 3 short + 3 long Mo–O bond distance distribution within the MoO_6 unit. Charge compensation is provided by interlayer NH_4^+ or Cs^+ cations. Powder X-ray, infrared, Raman and thermogravimetric data for these phases are also presented and discussed. The $M_2(MoO_3)_3SeO_3$ (M = NH_4, Cs) structure is related to, but distinctly different from the structure of $NH_4(VO_2)_3(SeO_3)_2$ recently reported. Crystal data: $(NH_4)_2(MoO_3)_3SeO_3$, M_r = 594.85, hexagonal, space group $P6_3$ (No. 173), a = 7.267(2) Å, c = 12.031(3) Å, V = 550.3(3) Å^3, Z = 2, R = 3.26%, R_w = 5.61% [559 observed reflections with $I > 3\sigma(I)$]; $Cs_2(MoO_3)_3SeO_3$, M_r = 824.58, hexagonal, space group $P6_3$ (No. 173), a = 7.312(2) Å, c = 12.377(2) Å, V = 573.1(3) Å^3, Z = 2, R = 5.93%, R_w = 6.52% [514 observed reflections with $I > 3\sigma(I)$].

Introduction

Relatively little is known about materials containing molybdenum cations in combination with selenite (SeO_3^{2-}) ions, which contrasts with the remarkable variety of molybdenophosphate materials that have been reported over the last few years.[1] The crystal structure of the molecular molybdenoselenite phase $(NH_4)_4Mo_5Se_2O_{21}\cdot 4H_2O$, consisting of discrete 5-rings of $Mo^{VI}O_6$ octahedra bi-capped by SeO_3 groups, was reported,[2] and $K_2Se_2MoO_8\cdot 3H_2O$, which contains a "polymeric" $[Se_2MoO_8]_n^{2n-}$ chain, has recently been characterized as the product of a hydrothermal reaction.[3]

We are now exploring the solid-state chemistry of the $M/Mo^{VI}/SeO_3$ phase space: Here we report the syntheses, noncentrosymmetric crystal structures, and some properties of the isostructural layered materials $(NH_4)_2(MoO_3)_3SeO_3$ and $Cs_2(MoO_3)_3SeO_3$. These materials are built up from hexagonal-WO_3-type sheets (Figure 1),[4] and are related to, but are *not* isostructural with $NH_4(VO_2)_3(SeO_3)_2$, a novel layered ammonium vanadium selenite.[5]

Experimental Section

Synthesis. *Caution*! Avoid toxic SeO_2 dust contamination with all appropriate safety measures. Single-phase, light yellow, hexagonal crystals of $(NH_4)_2(MoO_3)_3SeO_3$ (~65% yield based on molybdenum) were prepared from a reaction of starting composition 2.0 g $(NH_4)_6Mo_7O_{24}\cdot 4H_2O$, 0.632 g of SeO_2, and 4 mL of deionized water (NH_4:Mo:Se ratio = 1.71:2:1). This mixture was heated to 200 °C in a 23-mL capacity Teflon-lined Parr hydrothermal bomb for 48 h and then cooled to 40 °C over 24 h. Yellow crystals, of maximum linear dimension ~1 mm, were recovered by vacuum filtration (*pH* of filtrate = 5.3).

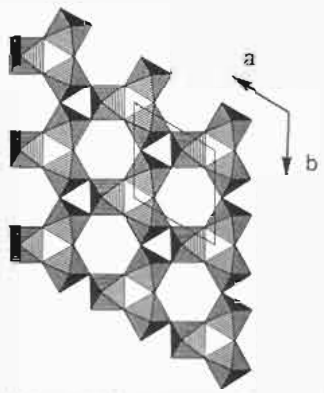

Figure 1. *STRUPLO* polyhedral view of a hexagonal tungsten bronze (HTB) octahedral layer, viewed down the crystallographic [001] direction, perpendicular to the layers. The linkage scheme for the apical oxygen atoms defines the dimensionality of the structure (see text).

Reactions which increased the amount of SeO_2 relative to that of $(NH_4)_6Mo_7O_{24}\cdot 4H_2O$ led to lower final pH's, and sharply reduced yields of $(NH_4)_2(MoO_3)_3SeO_3$: A synthesis at a starting NH_4:Mo:Se molar ratio of 1.71:2:4 only resulted in a 2% yield of $(NH_4)_2(MoO_3)_3SeO_3$ (pH 1.7).

Pure $Cs_2(MoO_3)_3SeO_3$ was prepared from a stoichiometric mixture of 0.358 g of $CsCO_3$, 0.475 g of MoO_3, 0.142 g of H_2SeO_3, and 4 mL of deionized water (Cs:Mo:Se ratio = 2:3:1). Hydrothermal reaction (23-mL Parr bomb, 2 days at 200 °C, slow cool overnight) led to small, platy, translucent, very light yellow crystals of $Cs_2(MoO_3)_3SeO_3$ (maximum linear dimension ~0.2 mm; ~94% yield based on Mo; pH of filtrate = 2.4).

Syntheses at molar ratios other than 2:3:1 for Cs:Mo:Se changed the resulting pH, yield and crystal size of $Cs_2(MoO_3)_3SeO_3$ product. Reactions which started with excess $CsCO_3$ (Cs:Mo:Se ratio = 2:1:1) led to lower yields of $Cs_2(MoO_3)_3SeO_3$ (~71% yield at pH 7.1). At a 2:1:1 starting ratio of Cs:Mo:Se, the yield of $Cs_2(MoO_3)_3SeO_3$ was almost quantitative, but the crystals recovered were intergrown and much smaller than those obtained from the 2:3:1 reaction, and unsuitable for single-crystal structure analysis. Reactions carried out at 180 °C produced off-white $Cs_2(MoO_3)_3SeO_3$ powder.

X-ray Powder Data. Diffraction data for crushed samples of $(NH_4)_2(MoO_3)_3SeO_3$ and $Cs_2(MoO_3)_3SeO_3$ were recorded on a Scintag

[⊗] Abstract published in *Advance ACS Abstracts*, November 15, 1994.

(1) Haushalter, R. C.; Mundi, L. A. *Chem. Mater.* **1992**, *4*, 31 and included references.
(2) Ichida, H.; Fukushima, H.; Sasaki, Y. *Nippon Kigaku Kaishi* **1986**, *11*, 1521.
(3) Robl, C.; Haake, K. *J. Chem. Soc., Chem. Commun.* **1992**, 1786.
(4) Gérand, B.; Nowogrocki, G.; Guenot, J.; Figlarz, M. *J. Solid State Chem.* **1979**, *29*, 429.
(5) Vaughey, J. T.; Harrison, W. T. A.; Dussack, L. L.; Jacobson, A. J. *Inorg. Chem.* **1994**, *33*, 4370.

0020-1669/94/1333-6043$04.50/0

Table 1. X-Ray Powder Data for $(NH_4)_2(MoO_3)_3SeO_3$

h	k	l	d_{obs} (Å)	d_{calc} (Å)	Δd (Å)[a]	I_{rel}[b]
1	0	0	6.297	6.294	0.003	31
0	0	2	6.016	6.016	0.000	39
1	0	1	5.575	5.577	−0.002	15
1	0	2	4.338	4.349	−0.011	1
1	1	0	3.636	3.634	0.002	3
1	0	3	3.383	3.382	0.001	6
2	0	0	3.151	3.147	0.004	6
1	1	2	3.110	3.110	0.000	13
2	0	1	3.043	3.045	−0.001	83
0	0	4	3.007	3.008	−0.001	66
2	0	2	2.790	2.788	0.002	23
1	0	4	2.716	2.714	0.002	100
2	0	3	2.476	2.476	0.000	6
2	1	0	2.379	2.379	0.000	2
1	2	1	2.334	2.334	0.000	2
1	0	5	2.248	2.248	0.000	6
1	2	2	2.212	2.212	0.000	3
3	0	1	2.066	2.067	−0.001	21
1	2	3	2.046	2.046	0.000	2
1	1	5	2.006	2.006	0.000	6
3	0	2	1.981	1.981	0.000	30
2	0	5	1.911	1.912	0.000	14
2	1	4	1.866	1.866	0.000	2
2	2	0	1.817	1.817	0.000	4
1	1	6	1.755	1.756	−0.001	8
2	2	2	1.739	1.739	0.000	5
1	3	1	1.727	1.728	0.000	4
1	2	5	1.692	1.692	0.000	3
1	3	2	1.677	1.676	0.000	5
1	0	7	1.659	1.658	0.001	16
1	3	3	1.601	1.601	0.000	4
2	2	4	1.555	1.555	0.000	10

[a] $d_{obs} - d_{calc}$. [b] $100\ I/I_{max}$.

XDS 2000 automated powder diffractometer ($\theta-\theta$ geometry, flat-plate sample, Cu Kα radiation, $\bar{\lambda} = 1.541\ 78$ Å, $T = 25(2)$ °C). The resulting patterns matched no known phases, including those of the starting materials. The instrumental Kα_1/Kα_2 profile was reduced to a single Cu Kα_1 peak ($\lambda = 1.540\ 568$ Å) by a software "stripping" routine, and d-spacings were established, relative to this wavelength. Prior to least-squares minimization of the lattice parameters, index-to-peak assignments were made on the basis of LAZY-PULVERIX[6] simulations using the single-crystal parameters described below. Optimized hexagonal cell parameters (with esd's in parentheses) of $a = 7.267(2)$ Å and $c = 12.033(3)$ Å ($V = 550.4(2)$ Å^3) were obtained for $(NH_4)_2(MoO_3)_3SeO_3$. Comparable values of $a = 7.314(3)$ Å and $c = 12.383(6)$ Å ($V = 573.7(4)$ Å^3) resulted for the $Cs_2(MoO_3)_3SeO_3$ refinement. Powder data for $(NH_4)_2(MoO_3)_3SeO_3$ and $Cs_2(MoO_3)_3SeO_3$ are reported in Tables 1 and 2, respectively.

Thermogravimetric Analysis. TGA data for $(NH_4)_2(MoO_3)_3SeO_3$ were collected on a TA Hi-RES TGA 2950 analyzer (ramp 2 °C per minute to 550 °C under flowing N_2 gas) and showed a fairly broad two-step weight loss of 16.3% at ~360 °C followed by another 11.5% weight loss at ~430 °C. X-ray powder diffraction showed the post-TGA residue to be pure orthorhombic MoO_3 (calculated weight loss for complete H_2O, NH_3, and SeO_2 elimination 27.4%; observed, 27.8%). An X-ray pattern of residue collected after heating to 340 °C showed the presence of both the orthorhombic and hexagonal[7a] forms of MoO_3 (this latter phase is described as "$(NH_4)_2O{\cdot}Mo_{22}O_{66}$" in the powder diffraction file[7b]). Hexagonal MoO_3 is *not* isostructural with *hex*-WO_3,[4] but consists of a three-dimensional array of corner- and edge-sharing MoO_6 groups, which form one-dimensional [001] tunnels.[7a]

TGA for $Cs_2(MoO_3)_3SeO_3$, collected under the same conditions, showed a one-step weight loss over the broad range ~320−540 °C, resulting in a residue of $Cs_2Mo_3O_{10}$[8] (calculated weight loss for total SeO_2 elimination = 13.5%; observed = 13%). The $Cs_2Mo_3O_{10}$ structure is unknown.

Table 2. X-Ray Powder Data for $Cs_2(MoO_3)_3SeO_3$

h	k	l	d_{obs} (Å)	d_{calc} (Å)	Δd (Å)[a]	I_{rel}[b]
0	0	2	6.191	6.192	−0.001	51
1	0	2	4.426	4.428	−0.001	6
1	1	0	3.658	3.657	0.001	59
1	0	3	3.456	3.458	−0.002	100
1	1	2	3.150	3.149	0.002	59
0	0	4	3.096	3.096	0.000	97
2	0	1	3.068	3.068	−0.001	70
1	0	4	2.782	2.781	0.001	48
1	0	5	2.308	2.307	0.002	27
0	0	6	2.062	2.064	−0.002	82
3	0	2	1.998	1.998	0.000	16
2	0	5	1.952	1.951	0.001	29
2	2	0	1.828	1.829	−0.001	15
2	0	6	1.729	1.729	0.000	15
1	3	3	1.616	1.616	0.000	17
4	0	1	1.571	1.571	0.000	18

[a] $d_{obs} - d_{calc}$. [b] $100\ I/I_{max}$.

Spectroscopic Data. Infrared spectra (KBr pellet method) for $(NH_4)_2(MoO_3)_3SeO_3$ and $Cs_2(MoO_3)_3SeO_3$ were measured from 400 to 4000 cm^{-1} on a Galaxy FTIR 5000 series spectrometer. Raman data were obtained using a coherent K-2 Kr^+ ion laser excited at 406.7 nm. Data for $(NH_4)_2(MoO_3)_3SeO_3$ and $Cs_2(MoO_3)_3SeO_3$ (KBr pellet method) were accumulated at one second intervals for every wavenumber over the range 100−1700 cm^{-1} (Spex 1403 double monochromator/Hamamatsu 928 photomultiplier detection system). At room temperature and 1 atm, the sample color changed from light yellow to grayish blue, indicating some surface damage upon irradiation.

Powder-second-harmonic-generation (PSHG) measurements (relative to a standard quartz signal)[9] made on well-ground samples of $(NH_4)_2(MoO_3)_3SeO_3$ and $Cs_2(MoO_3)_3SeO_3$ gave nonzero responses, indicating that both these materials crystallize in a noncentrosymmetric space group.

Reactivity Studies. Reactions of $(NH_4)_2(MoO_3)_3SeO_3$ with LiI under various conditions showed negligible evidence for any redox-intercalation or ion-exchange processes occurring, unlike the characteristic intercalation processes observed in layered $VOPO_4{\cdot}2H_2O$,[10] or the complex reactivity of $NH_4(VO_2)_3(SeO_3)_2$[5] with respect to reducing agents.

Crystal Structure Determination. The crystal structure of $(NH_4)_2(MoO_3)_3SeO_3$ was determined by standard single-crystal X-ray methods: A yellowish hexagonal prism (dimensions ~0.2 × 0.2 × 0.4 mm) was mounted on a thin glass fiber with epoxy, and room-temperature [25(2) °C] intensity data were collected on an Nicolet/Siemens automated 4-circle diffractometer (graphite-monochromated Mo Kα radiation, $\lambda = 0.710\ 73$ Å). After locating and centering 28 reflections ($18° < 2\theta < 30°$), we optimized the unit cell constants by least-squares refinement, resulting in hexagonal lattice parameters of $a = 7.267(2)$ Å and $c = 12.031(3)$ Å (esd's in parentheses). Intensity data were collected in the $\omega-2\theta$ scanning mode with standard reflections monitored for intensity changes throughout the course of the experiment (<±2% variation observed). The scan speed varied from 1.5 to 14.65°/min, for a total of 686 data collected ($2\theta < 60°$). During data reduction, an absorption correction based on ψ-scans (minimum 5.03, maximum 5.78) was applied to the data, and the normal corrections for Lorentz and polarization effects were made. The systematic absence condition ($000l$, $l \neq 2n$) in the reduced data indicated space groups $P6_3$, $P6_3/m$, or $P6_322$. Test data-merges indicated that Laue class $6/m$ was probably the correct one.

The crystal-structure model of $(NH_4)_2(MoO_3)_3SeO_3$ was developed in space group $P6_3$, with initial heavy-atom positions (Mo, Se) located by using the direct-methods program SHELXS-86.[11] No reasonable starting configuration could be established in space-group $P6_3/m$, which is consistent with the nonzero PSHG response of $(NH_4)_2(MoO_3)_3SeO_3$, and $P6_3$ was assumed for the remainder of the crystallographic analysis.

(6) Yvon, K.; Jeitschko, W.; Parthe, E. *J. Appl. Crystallogr.* **1977**, *10*, 73.
(7) (a) Olenkova, I. P.; Plyasova, L. M.; Kirik, S. D. *React. Kinet. Catal. Lett.* **1981**, *16*, 81. (b) JCPDS Powder Diffraction File, Card No. 26−78.
(8) Salmon, R.; Caillet, P. *Bull Soc. Chim. Fr.* **1969**, 1569.
(9) Dougherty, J. P.; Kurtz, S. K. *J. Appl. Crystallogr.* **1976**, *9*, 145.
(10) Jacobson, A. J.; Johnson, J. W.; Goshorn, D. P.; Merola, J. S. *Inorg. Chem.* **1985**, *24*, 1782.
(11) Sheldrick, G. M. *SHELXS-86* User Guide, Crystallography Department, University of Göttingen, Germany, 1986.

Table 3. Crystallographic Parameters

	$(NH_4)_2(MoO_3)_3SeO_3$	$Cs_2(MoO_3)_3SeO_3$
empirical formula	$Mo_3Se_1N_2O_{12}H_8$	$Cs_2Mo_3Se_1O_{12}$
fw	594.85	824.58
habit	hexagonal prism	hexagonal prism
color	off-yellow	very light yellow
cryst syst	hexagonal	hexagonal
a (Å)	7.267(2)	7.312(2)
c (Å)	12.031 (3)	12.377 (2)
V (Å^3)	550.3 (3)	573.1 (3)
Z	2	2
space group	$P6_3$ (No. 173)	$P6_3$ (No. 173)
T (°C)	25 (2)	25 (2)
λ(Mo Kα) (Å)	0.710 73	0.710 73
ϱ_{calc} (g/cm^3)	3.58	4.78
μ(Mo Kα) (cm^{-1})	66.31	125.79
tot no. data	686	1199
no. of obsd data[a]	559	517
hkl data limits	$-8\rightarrow0$, $0\rightarrow10$, $0\rightarrow16$	$-8\rightarrow0$, $0\rightarrow10$, $0\rightarrow17$
min, max $\Delta\varrho$ (e Å^{-3})	−3.7, +0.8	−4.3, +4.2
R^b (%)	3.26	5.93
R_w^c (%)	5.61	6.52

[a] $I > 3\sigma(I)$ after merging of equivalent data. [b] $R = 100\ \Sigma||F_o| - |F_c||/\Sigma|F_o|$. [c] $R_w = 100\ [\Sigma w(|F_o| - |F_c|)^2/\Sigma w|F_o|^2]^{1/2}$, with $w_i = 1/\sigma_i^2$.

The nitrogen and oxygen atom positions were located from Fourier difference maps during the refinement, and the refinement converged without any particular problems. The final cycles of full-matrix least-squares refinement were against F and included anisotropic temperature factors and a Larson-type secondary extinction correction[12] [refined value: 142(16)]. No H-atom positions could be determined from difference Fourier maps, and attempts at geometrical placement were ambiguous. Complex, neutral-atom scattering factors were obtained from ref 13. At the end of the refinement, analysis of the various trends in F_o versus F_c revealed no unusual effects. The least-squares, Fourier and subsidiary calculations were performed using the Oxford CRYSTALS system,[14] running on a DEC MicroVAX 3100 computer. Crystallographic data for $(NH_4)_2(MoO_3)_3SeO_3$ are summarized in Table 3.

The structure of $Cs_2(MoO_3)_3SeO_3$ was established in similar fashion: A transparent hexagonal plate, dimensions ~0.3 × 0.3 × 0.02 mm, was mounted on a thin glass rod with cyanoacrylate glue, and room-temperature [25(2) °C] intensity data were collected on an Enraf-Nonius CAD4 automated 4-circle diffractometer (graphite-monochromated Mo Kα radiation, λ = 0.710 73 Å). After locating and centering 25 reflections (15 ° < 2θ < 29°), we obtained optimized hexagonal unit-cell constants of a = 7.312(2) Å and c = 12.377(2) Å. Intensity data were collected in the $\omega-2\theta$ scanning mode: <±2% variation observed in intensity standards, scan speed = 1.5−14.7°/min, 1199 intensity maxima scanned, 2θ < 60°, systematic-absence condition (000l, $l \neq 2n$) indicated $P6_3$, $P6_3/m$, or $P6_322$. After data-merging (R_{Int} = 4.5%), 517 reflections were considered observed, according to the criterion $I > 3\sigma(I)$. Crystal absorption (minimum 1.55, maximum 3.21) was accounted for on the basis of ψ-scans.

Because of the similarity in lattice parameters and systematic absences between the ammonium and cesium phases, the structure of $Cs_2(MoO_3)_3SeO_3$ was refined in space group $P6_3$ using the $(NH_4)_2(MoO_3)_3SeO_3$ final atomic coordinates as a starting model (Cs substituting for N). The refinement converged satisfactorily: the final cycles of full-matrix refinement were against F and included anisotropic thermal factors (isotropic for oxygen) and a Larson secondary extinction correction [refined value: 6(2)]. Difference Fourier maps were noisier than expected, with several features close (<0.75 Å) to both the Mo and Se atom sites. Attempts to model these additional peaks as disorder of the Mo and Se atoms were not successful. A symmetry analysis of the $Cs_2(MoO_3)_3SeO_3$ structure, using the program MISSYM,[15] revealed considerable pseudo-symmetry, comparable with small atomic shifts of the Mo-, Se- and O-atoms from possible positions in space group $P6_3cm$. However, the $h\bar{h}0l$, $l \neq 2n$, absence condition consistent with $P6_3cm$ is strongly violated in the $Cs_2(MoO_3)_3SeO_3$ data. The nonzero SHG response observed eliminates the possibility of a centrosymmetric space group for $Cs_2(MoO_3)_3SeO_3$. At the end of the refinement (software: *CRYSTALS*), analysis of the various trends in F_o versus F_c revealed no unusual effects. Crystallographic data for $Cs_2(MoO_3)_3SeO_3$ are summarized in Table 3.

Table 4. Atomic Positional/Thermal Parameters for $(NH_4)_2(MoO_3)_3SeO_3$[b]

atom	x	y	z	U_{eq}[a]
N(1)	1/3	2/3	0.112(3)	0.0343
N(2)	1/3	2/3	−0.267(2)	0.0200
Mo(1)	0.3405(2)	0..1332(2)	0.8918(6)	0.0079
Se(1)	0	0	0.6559(6)	0.0090
O(1)	0.121(1)	−0.128(2)	0.905(1)	0.0116
O(2)	0.415(2)	0.205(2)	1.029(1)	0.0167
O(3)	0.548(2)	0.085(2)	0.847(1)	0.0115
O(4)	0.245(2)	0.126(2)	0.7210(9)	0.0116

[a] U_{eq} (Å^2) = $(U_1U_2U_3)^{1/3}$. [b] Protons not found.

Table 5. Bond Distances (Å) and Angles (deg) for $(NH_4)_2(MoO_3)_3SeO_3$

Mo(1)−O(1)	1.775(9)	Mo(1)−O(1)′	2.102(9)
Mo(1)−O(2)	1.73(1)	Mo(1)−O(3)	1.79(1)
Mo(1)−O(3)′	2.10(1)	Mo(1)−O(4)	2.16(1)
Se(1)−O(4) × 3	1.73(1)	N(1)−O(3) × 3	3.23(3)
N(1)−O(4) × 3	2.96(2)	N(2)−O(1) × 3	3.34(2)
N(2)−O(2) × 3	2.92(3)	N(2)−O(3) × 3	2.97(2)
O(1)−Mo(1)−O(1)′	88.7(6)	O(2)−Mo(1)−O(1)	102.3(6)
O(2)−Mo(1)−O(1)′	89.3(5)	O(3)−Mo(1)−O(1)	102.1(5)
O(3)−Mo(1)−O(1)′	163.6(5)	O(3)−Mo(1)−O(2)	100.3(5)
O(3)′−Mo(1)−O(1)	163.4(5)	O(3)′−Mo(1)−O(1)′	78.8(4)
O(3)′−Mo(1)−O(2)	88.6(5)	O(3)−Mo(1)−O(3)′	88.1(6)
O(4)−Mo(1)−O(1)	87.4(5)	O(4)−Mo(1)−O(1)′	77.9(5)
O(4)−Mo(1)−O(2)	163.9(5)	O(4)−Mo(1)−O(3)	90.1(5)
O(4)−Mo(1)−O(3)′	79.4(4)	O(4)−Se(1)−O(4)	101.1(5)
Mo(1)−O(1)−Mo(1)	149.4(6)	Mo(1)−O(3)−Mo(1)	134.4(6)
Se(1)−O(4)−Mo(1)	132.6(6)		

Results

Crystal Structure of $(NH_4)_2(MoO_3)_3SeO_3$. Final atomic positional and equivalent isotropic thermal parameters for $(NH_4)_2(MoO_3)_3SeO_3$ are listed in Table 4, with selected bond distance/angle data in Table 5. $(NH_4)_2(MoO_3)_3SeO_3$ is a new phase built up from ammonium ions and layers of vertex-sharing MoO_6 and SeO_3 units, which are connected *via* Mo−O−Mo and Mo−O−Se bonds. The Mo/Se/O asymmetric unit and labeling scheme of $(NH_4)_2(MoO_3)_3SeO_3$ is shown in Figure 2, and the complete crystal structure is illustrated in Figure 3.

The single, crystallographically-distinct molybdenum atom occupies a distorted octahedron, with a short "molybdyl" Mo−O bond to O(2) [d = 1.73(1) Å] which is not bound to any other atoms, four Mo−O−Mo bonds [*via* O(1) O(1)′, O(3) and O(3)′ (Table 5)], and one Mo−O−Se link, *via* O(4). The MoO_6 octahedron is distorted—the Mo cation is displaced by 0.33 Å from the geometrical center of its six oxygen atom neighbors, resulting in three "short" bonds [to O(1), O(2) and O(3)] with d(Mo−O) < 1.8 Å, each of which is *trans* to a "long" Mo−O bond (d > 2.1 Å) to O(1)′, O(3)′, and O(4) (Figure 4 and Table 5). This $Mo^{VI}O_6$ octahedral distortion mode is unusual, and is discussed below. A Brese−O'Keefe bond valence sum (BVS) calculation[16] for Mo(1) gave a value of 6.10, in good agreement with the expected value of 6.00. The selenium atom, Se(1),

(12) Larson, A. C. *Acta Crystallogr.* **1967**, *23*, 664.
(13) Cromer, D. T. *International Tables for X-Ray Crystallography*; Kynoch Press: Birmingham, England, 1974; Volume IV, Table 2.3.1.
(14) Watkin, D. J.; Carruthers, J. R.; Betteridge, P. W. CRYSTALS *User Guide*; Chemical Crystallography Laboratory, Oxford University: Oxford, U.K., 1993.
(15) Le Page, Y. *J. Appl. Crystallogr.* **1988**, *21*, 983.
(16) Brese, N.; O'Keefe, M. *Acta Crystallogr.* **1991**, *B47*, 192.

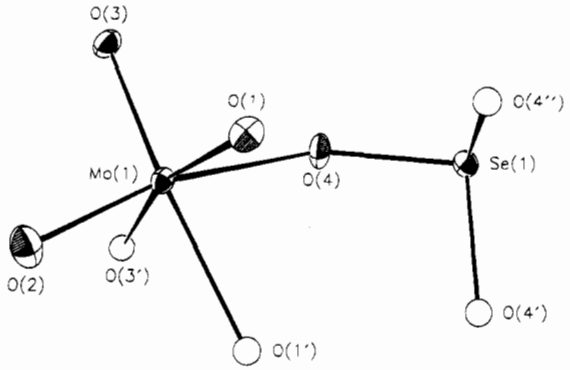

Figure 2. *ORTEP* view of the Mo/Se/O asymmetric unit of $(NH_4)_2(MoO_3)_3SeO_3$, showing the atom-labeling scheme (50% thermal ellipses).

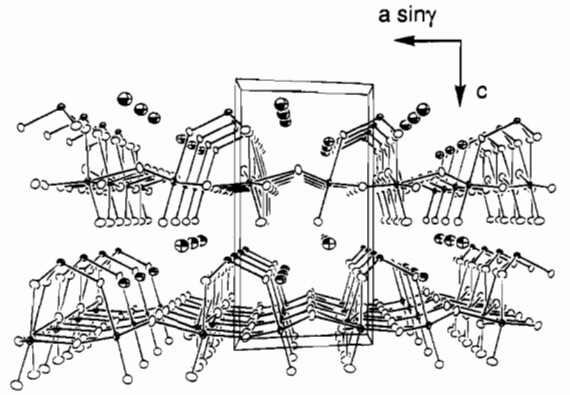

Figure 3. Unit cell packing of $(NH_4)_2(MoO_3)_3SeO_3$, viewed down [010], showing the Mo/Se/O sheet structure (N−O contacts not shown).

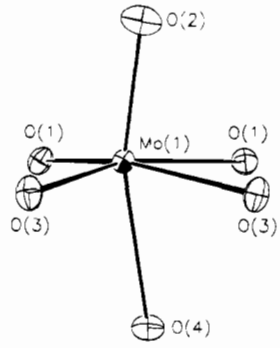

Figure 4. Detail of the Mo(1) coordination polyhedron in $(NH_4)_2(MoO_3)_3SeO_3$, showing the displacement of the Mo atom from the geometrical center of the MoO_6 octahedron.

occupies typical pyramidal coordination (BVS[Se(1)] = 3.73; site symmetry: 3) with three equivalent Se(1)−O(4) bonds, each of which bridges to a different MoO_6 unit (Figure 5), although the MoO_6 units are linked into a triangular unit as noted below. The four distinct oxygen atoms partake in Mo−O−Mo bridges [(O(1) and O(3); θ_{av} = 142°], an Mo−O(4)−Se link, and a terminal Mo−O(2) bond.

The two ammonium ions (nitrogen atoms) in $(NH_4)_2(MoO_3)_3SeO_3$ both occupy special positions with 3-fold symmetry. N(1) has six oxygen-atom neighbors within 3.5 Å, which form a distorted hexagon, on one side of the N atom (Figure 6); *i.e.*, all the N(1)···O contacts are to one distinct Mo/Se/O layer. N(2) bonds to nine O atoms within the same distance limit: three bonds to three equivalent O(2) atoms in one Mo/Se/O layer, and six bonds to a "chair" of O(1) and O(3) atoms (Figure 7) in the adjacent Mo/Se/O layer. Neither of these conformations results in unambiguous H-bonding schemes.

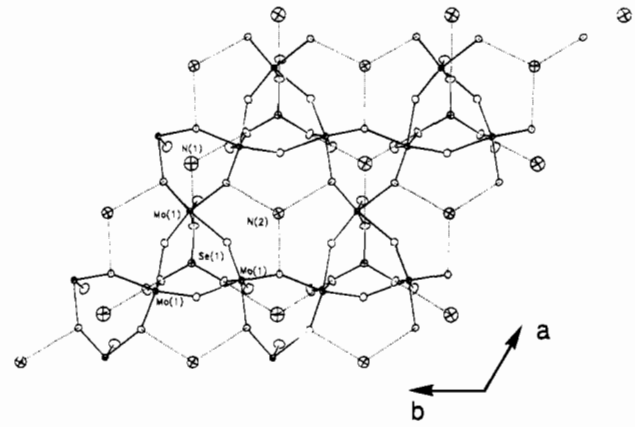

Figure 5. [001] slice of the crystal structure of $(NH_4)_2(MoO_3)_3SeO_3$ ($0.05 < z < 0.55$), showing the connections between MoO_6 octahedra, and capping Se-atoms.

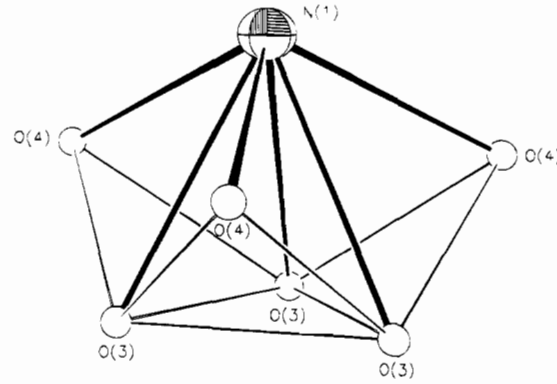

Figure 6. Detail of the N(1) coordination polyhedron in $(NH_4)_2(MoO_3)_3SeO_3$, with nonbonding O···O contacts < 4.0 Å indicated by thin lines. O atoms are represented by spheres of arbitrary radius.

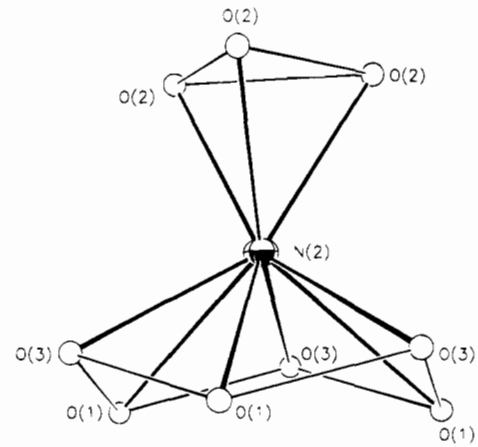

Figure 7. Detail of the N(2) coordination polyhedron in $(NH_4)_2(MoO_3)_3SeO_3$, with nonbonding O···O contacts < 4.0 Å indicated by thin lines. O atoms are represented by spheres of arbitrary radius.

The structural *motif* in $(NH_4)_2(MoO_3)_3SeO_3$ (Figure 5) consists of infinite sheets of vertex-sharing triangles of MoO_6 octahedra [linked *via* O(1) and O(3)], which are linked into hexagonal tungsten bronze (HTB) like layers, enclosing hexagonal "channels" (*cf.* Figure 1). The hexagonal *a* lattice constant of *hex*-WO_3[4] is 7.298 Å, almost identical to the 7.267 (2) Å found here for $(NH_4)_2(MoO_3)_3SeO_3$. In the layer configuration in $(NH_4)_2(MoO_3)_3SeO_3$, each MoO_6 octahedron shares four vertices with similar adjacent units; each Mo−O−Mo link comprises of a short (d < 1.8 Å) plus a long (d > 2.1 Å) molybdenum-oxygen bond. The oxygen atoms of the MoO_6 unit form a fairly regular octahedron, with an average O···O

Table 6. Atomic Positional Parameters for $Cs_2(MoO_3)_3SeO_3$

atom	x	y	z	U_{eq}[a]
Cs(1)	1/3	2/3	0.0964(3)	0.0250
Cs(2)	1/3	2/3	−0.2671(2)	0.0120
Mo(1)	0.3389(3)	0.1363(3)	0.8967(2)	0.0083
Se(1)	0	0	0.6699(4)	0.0052
O(1)	0.122(2)	−0.131(2)	0.911(2)	0.010(2)[b]
O(2)	0.407(3)	0.196(3)	1.031(2)	0.010(2)[b]
O(3)	0.544(3)	0.083(3)	0.856(1)	0.010(2)[b]
O(4)	0.243(3)	0.128(3)	0.732(1)	0.010(2)[b]

[a] U_{eq} (Å^2) = $(U_1U_2U_3)^{1/3}$. [b] U_{iso} (Å^2).

Table 7. Bond Distances (Å) and Angles (deg) for $Cs_2(MoO_3)_3SeO_3$

Mo(1)−O(1)	1.81(1)	Mo(1)−O(1)	2.09(1)
Mo(1)−O(2)	1.72(2)	Mo(1)−O(3)	1.80(2)
Mo(1)−O(3)	2.11(2)	Mo(1)−O(4)	2.15(2)
Se(1)−O(4) × 3	1.72(2)	Cs(1)−O(1) × 3	3.49(2)
Cs(1)−O(4) × 3	3.16(2)	Cs(2)−O(1) × 3	3.42(2)
Cs(2)−O(2) × 3	3.00(2)	Cs(2)−O(3) × 3	3.05(2)
O(1)−Mo(1)−O(1)′	90.4(8)	O(1)−Mo(1)−O(2)	99.6(9)
O(1)−Mo(1)−O(2)	89.6(9)	O(1)−Mo(1)−O(3)	99.8(7)
O(1)−Mo(1)−O(3)	165.2(8)	O(2)−Mo(1)−O(3)	99.1(9)
O(1)−Mo(1)−O(3)	165.9(8)	O(1)−Mo(1)−O(3)	79.2(6)
O(2)−Mo(1)−O(3)	89.8(8)	O(3)−Mo(1)−O(3)′	88.9(10)
O(1)−Mo(1)−O(4)	87.9(8)	O(1)−Mo(1)−O(4)	78.3(8)
O(2)−Mo(1)−O(4)	165.8(7)	O(3)−Mo(1)−O(4)	91.3(8)
O(3)−Mo(1)−O(4)	80.8(7)	O(4)−Se(1)−O(4)′	101.7(8)
Mo(1)−O(1)−Mo(1)′	147.5(9)	Mo(1)−O(3)−Mo(1)′	135.7(1)
Mo(1)−O(4)−Se(1)	132.2(10)		

distance of 2.72 Å (minimum = 2.67 Å, maximum = 2.81 Å); thus the Mo−O−Mo bond length alternation may be considered to arise from displacement of the molybdenum atom inside the MoO_6 group toward one of the MoO_6 octahedral faces. The two apical oxygen atoms of the MoO_6 group, O(2) and O(4), both project into the intersheet region, forming isolated "triangles" of three Mo−O bonds. Half of these molybdenum-oxygen triangles are "capped" by selenium atoms, all of which are on one face of the Mo/O sheet, whereas the apical Mo−O bonds on the other side of the Mo/O sheet have no capping atoms. There are no inter-sheet bonds, except those bridged by the ammonium cation, N(2), as indicated above.

Crystal Structure of $Cs_2(MoO_3)_3SeO_3$. Final atomic positional and equivalent isotropic thermal parameters for $Cs_2(MoO_3)_3SeO_3$ are listed in Table 6, with selected bond distance/angle data in Table 7. $Cs_2(MoO_3)_3SeO_3$ is isostructural with $(NH_4)_2(MoO_3)_3SeO_3$, and contains similar Mo/Se/O layers, (connected *via* Mo−O−Mo and Mo−O−Se bonds) sandwiching Cs^+ cations.

The molybdenum atom in $Cs_2(MoO_3)_3SeO_3$ occupies a distorted octahedron, with a short Mo−O(2) bond [d = 1.72 (2) Å], four Mo−O−Mo bonds *via* O(1) O(1)′, O(3), and O(3)′ (Table 7), and a Mo−O(4)−Se link. The distortion mode of the MoO_6 octahedron in $Cs_2(MoO_3)_3SeO_3$ is very similar to that found in the equivalent unit in $(NH_4)_2(MoO_3)_3SeO_3$, resulting in three short bonds (d < 1.82 Å) each of which are *trans* to a long (d > 2.08 Å) Mo−O link. The displacement of the Mo atom from the geometrical center of its six oxygen atom neighbors is 0.30 Å, and, as with $(NH_4)_2(MoO_3)_3SeO_3$, may be viewed as a local [111] displacement, toward an octahedral *face*. The oxygen atoms around Mo(1) form a fairly regular octahedron (O···O contacts: minimum = 2.676 Å, average = 2.73 Å, maximum 2.84 Å). A BVS[Mo(1)] of 6.00 results for this polyhedron, as expected for Mo^{VI}. The selenium atom (BVS = 3.84, site symmetry: 3) makes three equivalent Se(1)−O(4) bonds, each of which bridges to a different MoO_6 unit.

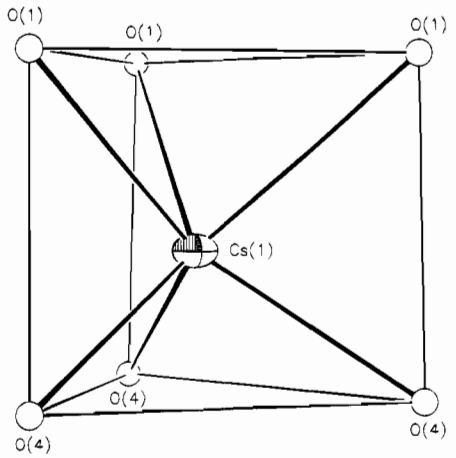

Figure 8. Detail of the Cs(1) coordination polyhedron in $Cs_2(MoO_3)_3SeO_3$, with nonbonding O···O contacts < 4.0 Å indicated by thin lines. O atoms are represented by spheres of arbitrary radius.

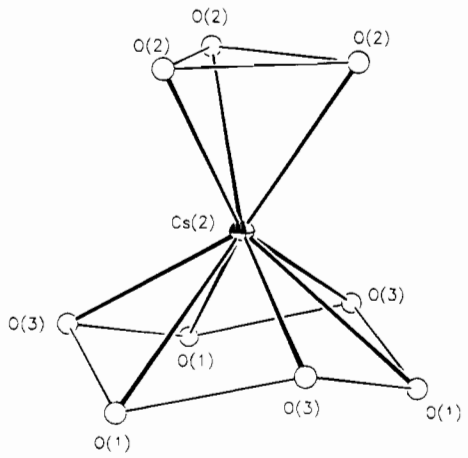

Figure 9. Detail of the Cs(2) coordination polyhedron in $Cs_2(MoO_3)_3SeO_3$, with nonbonding O···O contacts < 4.0 Å indicated by thin lines. O atoms are represented by spheres of arbitrary radius.

The two cesium cations in $Cs_2(MoO_3)_3SeO_3$ both occupy special positions (site symmetry: 3). Cs(1) makes six bonds to nearby oxygen atoms within 3.5 Å, forming a trigonal prism, as shown in Figure 8. Cs(2) bonds to nine O atoms within the same distance limit: three bonds to three equivalent O(2) atoms in one Mo/Se/O layer, and six bonds to a "chair" of O(1) and O(3) atoms (Figure 9) in the adjacent Mo/Se/O layer. Cs(2) in $Cs_2(MoO_3)_3SeO_3$, and N(2) in $(NH_4)_2(MoO_3)_3SeO_3$ (*vide supra*), have very similar coordinations: however, Cs(1) is shifted further into the interlayer region in $Cs_2(MoO_3)_3SeO_3$ than the equivalent N(1) in $(NH_4)_2(MoO_3)_3SeO_3$. This shifting, by about 0.2 Å, may be due to the hydrogen-bonding preference of the $N(1)H_4$ group in $(NH_4)_2(MoO_3)_3SeO_3$, *versus* the more symmetrical bonding requirements of the Cs^+ cation in $Cs_2(MoO_3)_3SeO_3$.

Physical and Spectroscopic Measurements. The IR spectrum of $(NH_4)_2(MoO_3)_3SeO_3$ (Figure 10a) shows four prominent bands for the tetrahedral NH_4 cation, three at 3160, 3020, and 2800 cm^{-1} (symmetric ν_1 and asymmetric ν_3 stretches) and a sharp band at 1412 cm^{-1} (asymmetric ν_4 stretch). The ammonium bands are absent from the spectrum of $Cs_2(MoO_3)_3SeO_3$ (Figure 10b), and there are no signals attributable to water for either material. Both the $(NH_4)_2(MoO_3)_3SeO_3$ and $Cs_2(MoO_3)_3SeO_3$ spectra show IR bands associated with octahedral MoO_6 groups. For $(NH_4)_2(MoO_3)_3SeO_3$, strong, broad bands at 698 and 673 cm^{-1} and sharp bands at 937 and 876 cm^{-1} are observed. The characteristic frequencies associated

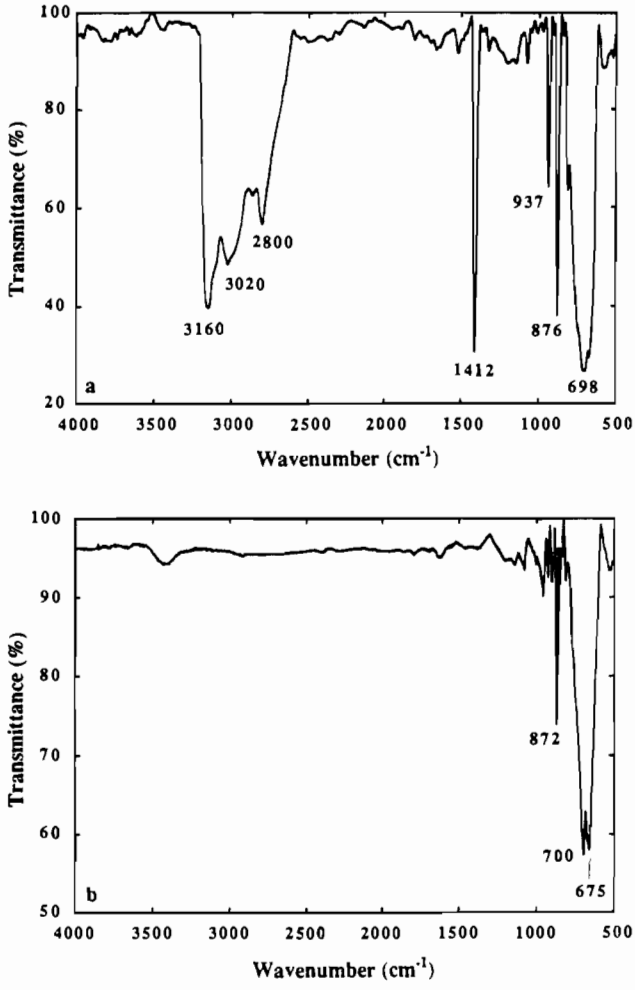

Figure 10. IR spectra of (a, top) $(NH_4)_2(MoO_3)_3SeO_3$ and (b, bottom) $Cs_2(MoO_3)_3SeO_3$.

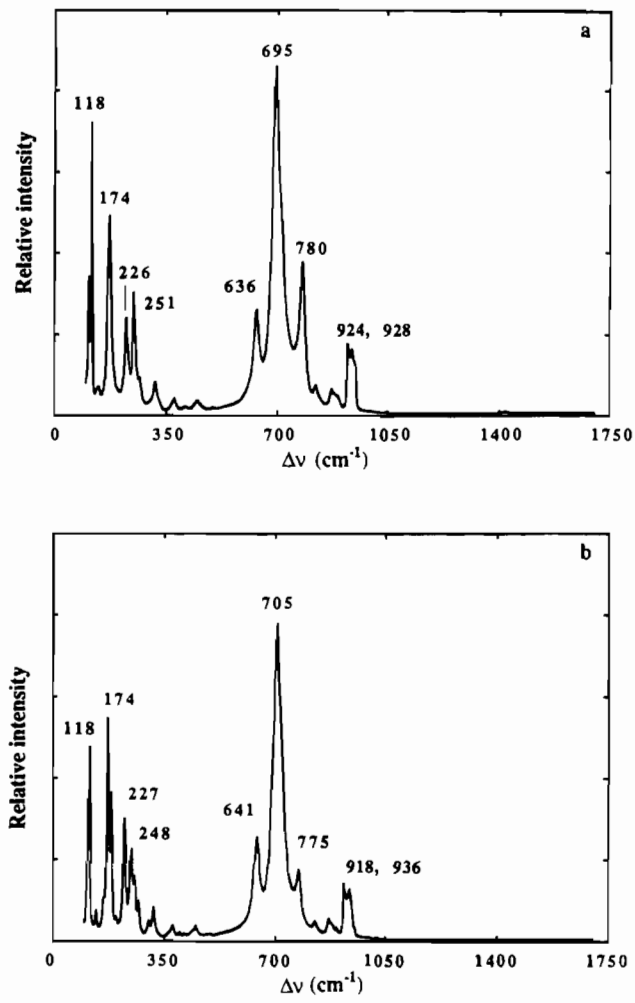

Figure 11. Raman spectra of (a, top) $(NH_4)_2(MoO_3)_3SeO_3$ and (b, bottom) $Cs_2(MoO_3)_3SeO_3$.

with Mo−O and Se−O[17] stretches are expected to occur in the region 600−900 cm^{-1}, and the corresponding bands in $Cs_2(MoO_3)_3SeO_3$ are at very similar locations. The broad band at ~700 cm^{-1} is probably due to Mo−O stretches.

The Raman spectra of $(NH_4)_2(MoO_3)_3SeO_3$ and $Cs_2(MoO_3)_3SeO_3$ are shown in parts a and b of Figure 11 and are virtually identical in the region 400−1050 cm^{-1}. Peaks below ~350 cm^{-1} correspond to cooperative lattice (phonon) modes in these layered structures: similar features were observed in the detailed study of the spectroscopic properties of the related, layered, $K_3(SbO_2)_3(XO_4)_2{\cdot}xH_2O$ (X = P, As) structures.[19] Symmetric stretches for the MoO_6 and SeO_3 groups correspond to strong Raman bands, whereas the asymmetric stretches are weak. For the $(NH_4)_2(MoO_3)_3SeO_3$ spectrum, the intense peak at 695 cm^{-1} corresponds to a stretching mode for MoO_6, and corresponds to a prominent IR band for the same material (Figure 10a). For $Cs_2(MoO_3)_3SeO_3$, a similar correspondence is observed between strong Raman and IR bands. The SeO_3 group has a sharp, pronounced peak at 780 cm^{-1} for $(NH_4)_2(MoO_3)_3SeO_3$ and at 775 cm^{-1} for $Cs_2(MoO_3)_3SeO_3$, corresponding to the intense Raman band observed previously observed at 781 cm^{-1} for the SeO_3 group in $NH_4(VO_2)_3(SeO_3)_2$.[5]

Conclusions

$(NH_4)_2(MoO_3)_3SeO_3$ and $Cs_2(MoO_3)_3SeO_3$ are new, noncentrosymmetric layered structures, whose layer *motif* is based on a slice of the hexagonal tungsten bronze structure.[4,18] Unlike tungsten bronzes, in which the WO_6 layers are interconnected by apical W−O−W′ links into a three-dimensional structure containing channels which may be (partially) occupied by other species,[18] the MoO_6 layers in $(NH_4)_2(MoO_3)_3SeO_3$ and $Cs_2(MoO_3)_3SeO_3$ are isolated. One side of the MoO_6 octahedral layers are capped by selenium atoms, while the other side of the sheet has no capping atoms, leading to a very asymmetric structure. $NH_4(VO_2)_3(SeO_3)_2$[5] has a similar layer of vanadium-centered octahedra, but in this material, *both* sides of the octahedral layer are capped by selenium atoms. Polyhedral plots (Figure 12) indicate the relationship between the two structure types. Potassium antimony phosphate/arsenate $K_3(SbO_2)_3(XO_4)_2{\cdot}xH_2O$ (X = P, As)[20] has a similar layer structure to $NH_4(VO_2)_3(SeO_3)_2$, and is built up from HTB layers of SbO_6 octahedra, capped on both sides by X−O (X = P, As) groups (as opposed to a Se atom for $NH_4(VO_2)_3(SeO_3)_2$ and the $M_2(MoO_3)_3SeO_3$ phases described here), although three, rather than two univalent cations are required for charge balancing in $K_3(SbO_2)_3(XO_4)_2{\cdot}xH_2O$, and water molecules are also included in the inter-layer region of this structure.

An important difference between these various layered phases may be observed in the distortion modes of the octahedrally-

(17) Morris, R. E.; Harrison, W. T. A.; Stucky, G. D.; Cheetham, A. K. *J. Solid State Chem.* **1991**, *94*, 227.
(18) Labbe, P. H.; Goreaud, M.; Raveau, B.; Monier, J. C. *Acta Crystallogr.* **1978**, *B34*, 1433.
(19) Husson, E.; Lachgar, A.; Piffard, Y. *J. Solid State Chem.* **1988**, *74*, 138.
(20) Lachgar, A.; Deniard-Courant, S.; Piffard, Y. *J. Solid State Chem.* **1988**, *73*, 572.

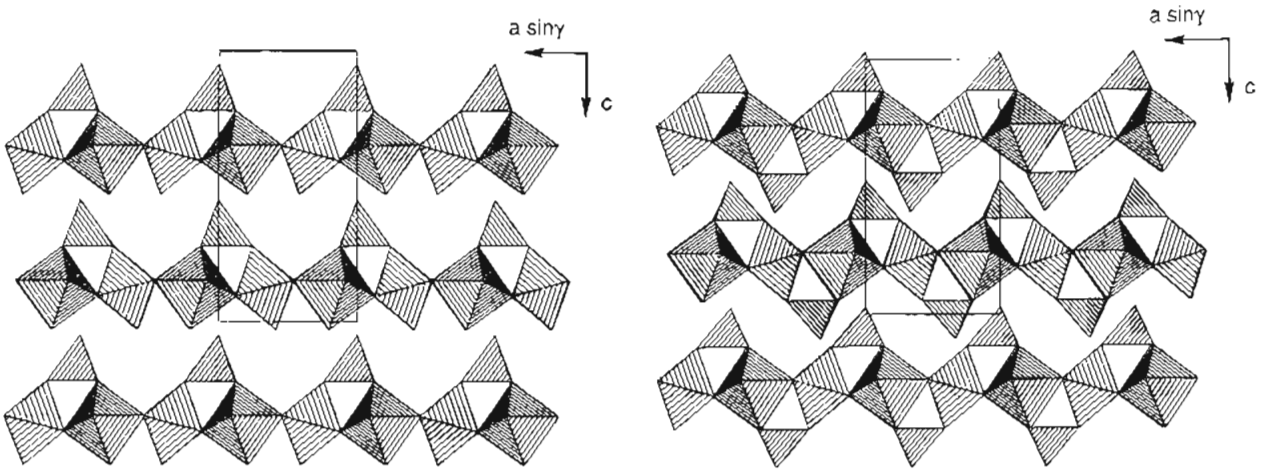

Figure 12. Polyhedral plots of the $M_2(MoO_3)_3SeO_3$ (left) and $NH_4(VO_2)_3(SeO_3)_2$ (right) structures, viewed down [010], with the selenite group represented by a tetrahedron. The fourth, unbonded vertex of the tetrahedron represents the lone pair of the Se atom. The MoO_6 layers in $M_2(MoO_3)_3SeO_3$ are capped on one side by Se, while the VO_6 layers in $NH_4(VO_2)_3(SeO_3)_2$ are capped on both sides by selenium atoms (see text and ref 5).

Table 8. Octahedral Bond Distance (Å) Distribution for *hex*-WO_3 Type Phases

Phase	S^a	M−O bond distances (shortest to longest)					
$(NH_4)_2(MoO_3)_3SeO_3$	1	1.73(1)	1.775(9)	1.79(1)	2.10(1)	2.102(9)	2.16(1)
$Cs_2(MoO_3)_3SeO_3$	1	1.72(2)	1.80(2)	1.81(1)	2.09(1)	2.11(2)	2.15(2)
$NH_4(VO_2)_3(SeO_3)_2$	1	1.64(1)	1.650(8)	1.927(9)	1.975(8)	2.181(8)	2.20(2)
$K_3(SbO_2)_3(PO_4)_2$	2/*m*	1.944(1)	1.944(1)	1.944(1)	1.944(1)	2.014(3)	2.014(3)
hex-WO_3	*mmm*	1.887	1.887	1.887	1.887	1.949	1.949
$Rb_{0.28}WO_3$	*m*2*m*	1.840	1.840	1.883	1.922	1.991	1.991
$Na_{1/2}(H_3O)_{1/2}Nb_2PO_8$[b]	1	1.834(5)	1.896(3)	1.933(3)	2.062(5)	2.091(4)	2.103(5)

[a] Crystallographic site symmetry of metal. [b] HTB layers contain octahedral "vacancies".[21]

coordinated atoms. In $(NH_4)_2(MoO_3)_3SeO_3$ and $Cs_2(MoO_3)_3SeO_3$, the molybdenum atom inside the MoO_6 octahedron is displaced toward an octahedral face ("three long + three short" Mo−O bonds), whereas in $NH_4(VO_2)_3(SeO_3)_2$,[5] the vanadium atom tends towards an octahedral *edge*, resulting in an unusual two long + two intermediate + two short V−O bond-length distribution. Conversely, in $K_3(SbO_2)_3(PO_4)_2{\cdot}5H_2O$,[20] the SbO_6 group is almost regular, with no identifiable short or long Sb−O bonds. In *hex*-WO_3[4] and $Rb_{0.28}WO_3$,[18] the WO_6 octahedron is also close to being regular, and no distinct, short W−O bonds are apparent. The phase $Na_{1/2}(H_3O)_{1/2}Nb_2PO_8$[21] has a "defect" WO_3 type structure, in which some of the NbO_6 octahedra are replaced by tetrahedral PO_4 groups. $Na_{1/2}(H_3O)_{1/2}Nb_2PO_8$ (Table 8) shows a similar three short + three long Nb−O bond-length configuration within the NbO_6 octahedron, and displays a significant PSHG response of ~100 × quartz.[21] These octahedral bond-distance data are summarized in Table 8. It is apparent that the octahedral distortion mode (along a bond, toward an edge, toward a face) is highly dependent on the precise nature of the phase in question, and probably depends on the nature of the neighboring atoms, as well as the first coordination sphere of oxygen atoms about the octahedrally-coordinated cation. This second-order effect cannot be directly correlated with electron configurations of the octahedral cations.

Our synthetic and structural studies of layered HTB-like materials containing other cations and capping groups are continuing, and will be reported later.

Acknowledgment. We thank Jim Korp and Ivan Bernal for assistance with the X-ray data collections and Paul Meloni and Roman Czernuszewicz for assistance in collecting the Raman data. Vojislav Srdanov (UC Santa Barbara) kindly collected the PSHG data. This work was funded by the National Science Foundation (DMR-9214804) and the Robert A. Welch Foundation.

Supplementary Material Available: Tables of anisotropic thermal parameters for $(NH_4)_2(MoO_3)_3SeO_3$ and $Cs_2(MoO_3)_3SeO_3$ (1 page). Ordering information is given on any current masthead page.

(21) Liang, C. S.; Harrison, W. T. A.; Eddy, M. M.; Gier, T. E.; Stucky, G. D. *Chem. Mater.* **1993**, *5*, 917.